Tectonophysics, 155 (1988) 1–26
Elsevier Science Publishers B.V., Amsterdam – Printed in The Netherlands

Tectonic fabric map of the ocean basins from satellite altimetry data

L.M. GAHAGAN [1], C.R. SCOTESE [2], J.-Y. ROYER [3], D.T. SANDWELL [3], J.K. WINN [1], R.L. TOMLINS [1], M.I. ROSS [1], J.S. NEWMAN [1], R.D. MÜLLER [4], C.L. MAYES [1], L.A. LAWVER [3] and C.E. HEUBECK [1]

[1] *The Department of Geological Sciences, The University of Texas, Austin, TX 78713 (U.S.A.) and The Institute for Geophysics, The University of Texas, 8701 Mopac Boulevard, Austin, TX 78759 (U.S.A.)*
[2] *Shell Development Co., Bellaire Research Center, P.O. Box 481, Houston, TX 77001 (U.S.A.)*
[3] *The Institute for Geophysics, The University of Texas, 8701 Mopac Boulevard, Austin, TX 78759 (U.S.A.)*
[4] *Geologisch- Paläontologisches Institut und Museum der Christian-Albrechts Universität Kiel, Olshausenstrasse 40, D-2300 Kiel 1 (F.R.G.)*

(Received April 10, 1987; revised version accepted March 4, 1988)

Abstract

Gahagan, L.M., Scotese, C.R., Royer, J.-Y., Sandwell, D.T., Winn, J.K., Tomlins, R.L., Ross, M.I., Newman, J.S., Müller, R.D., Mayes, C.L., Lawver, L.A. and Heubeck, C.E., 1988. Tectonic fabric map of the ocean basins from satellite altimetry data. In: C.R. Scotese and W.W. Sager (Editors), Mesozoic and Cenozoic Plate Reconstructions. *Tectonophysics*, 155:1–26

Satellite altimetry data provide a new source of information on the bathymetry of the ocean floor. The tectonic fabric of the oceans (i.e., the arrangement of fracture zones, ridges, volcanic plateaus and trenches) is revealed by changes in the horizontal gravity gradient as recorded by satellite altimetry measurements. SEASAT and GEOSAT altimetry data have been analyzed and a global map of the horizontal gravity gradient has been produced that can be used to identify a variety of marine tectonic features. The uniformity of the satellite coverage provides greater resolution and continuity than maps based solely on ship-track data. This map is also the first global map to incorporate the results of the GEOSAT mission, and as a result, new tectonic features are revealed at high southerly latitudes.

This map permits the extension of many tectonic features well beyond what was previously known. For instance, various fracture zones, such as the Ascension, Tasman, and Udintsev fracture zones, can be extended much closer to adjacent coninental margins. The tectonic fabric map also reveals many features that have not been previously mapped. These features include extinct ridges, minor fracture zone lineations and seamounts. In several areas, especially across aseismic plateaus or along the margins of the continents, the map displays broad gravity anomalies whose origin may be related to basement structures.

Introduction

During the past decade, remote sensing data obtained from orbiting satellites have provided new information about geology at the Earth's surface (LANDSAT) and the structure of the Earth's magnetic (MAGSAT) and gravity fields (SEASAT and GEOSAT). The geoid is an equipotential gravitational surface that is closely approximated by the sea surface. The shapes of the geoid and sea surface change in response to gravitational anomalies within the Earth. The long-wavelength signals (> 1000 km) of the geoid are due to structures deep within the Earth while the short-wavelength signals (~ 200 km or less) are the result of mass excesses and deficits near the surface. In areas of excess mass, such as in the vicinity of an oceanic ridge or seamount, there are

0040-1951/88/$03.50

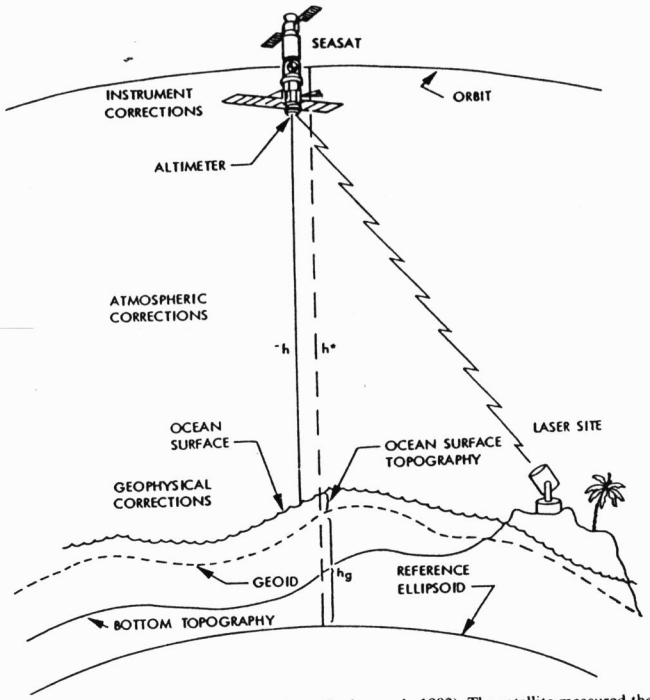

Fig. 2. Schematic diagram of the SEASAT satellite in orbit (from Tapley et al., 1982). The satellite measured the distance (h) between itself and the sea surface using a radar altimeter. Ground-tracking lasers located the satellite in its orbit, permitting the calculation of the distance (h^*) between the satellite and a reference ellipsoid around the Earth. Correction for various factors (instrument and atmosphere) were made to the data. The height of the sea surface is equal to the difference between h^* and h.

In order to ensure the accuracy of the SEASAT data, the Jet Propulsion Laboratory, in conjunction with NASA, formed the SEASAT Altimeter–Precision Orbit Determination Experiment Team. Using correction algorithms (Hancock et al., 1980, Lorell, 1980; Parke et al., 1980) and in situ surface gravity measurements the team was able to verify the accuracy and resolution of the SEASAT measurements (Lame and Born, 1982; Tapley et al., 1982). Corrections were made for instrumentation, orbit, temporal variations and other secular effects. Among its conclusions, the team was able to determine that the altimetry measurements between the satellite and sea surface were accurate to within 10 cm for wave heights of less than 20 m as determined by the satellite (Tapley et al., 1982).

On March 12, 1985, the geodesy satellite, or GEOSAT was launched by the U.S. Navy in order to complete SEASAT's mission and obtain a high-resolution, global-scale, oceanographic data set. The John Hopkins Applied Physics Laboratory (APL) constructed the satellite and is responsible for its operation (Mitchell et al., 1987). During its 18 month, primary mission, GEOSAT made over 270 million observations along an orbital track of 200 million km. The orbits repeated approximately every 3 days and the tracks had an equatorial spacing of 4 km (Jenson and Wooldridge, 1987; McConathy and Kilgus, 1987; Mitchell et al., 1987). On October 1, 1986, GEOSAT began its secondary mission of collecting unclassified oceanographic data along a 17 day repeat orbit with 164 km equatorial-spaced ground

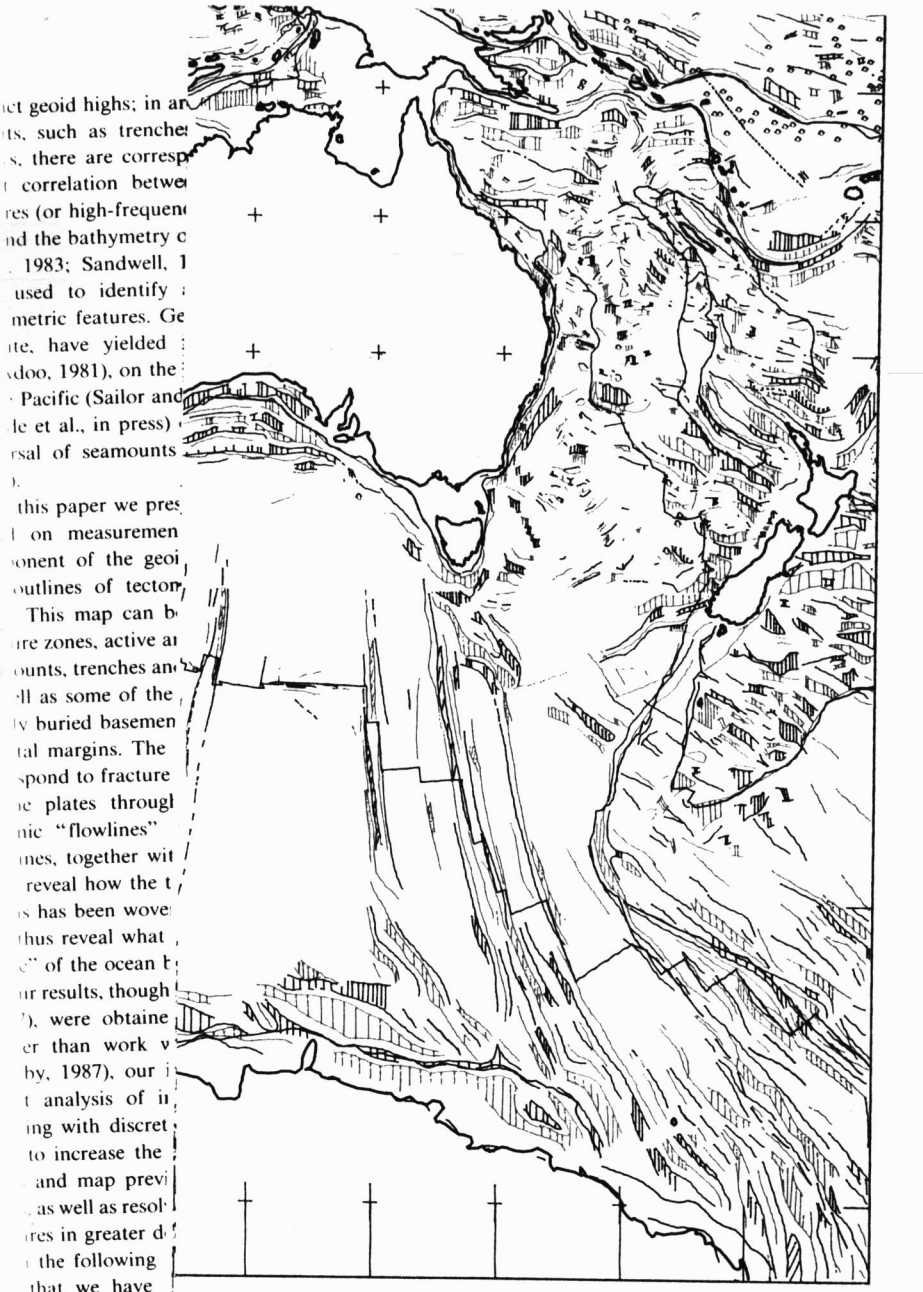

ıd GEOSAT) altimetry data. The map should be read from south to north. The blue lineations
ns represent negative gravity gradients (or slopes in the sea surface). For instance, crossing a blue
oing downslope. Although the tectonic fabric map is dominated by linear flowlines corresponding
es, such as ridges and aseismic plateaus, can be identified.

s. Using an altimeter similar to SEASAT's,)SAT measured the height of the sea surface n accuracy of 3.5 cm for significant wave its of 2 m (MacArthur et al., 1987; McCon- and Kilgus, 1987). GEOSAT data can resolve res with wavelengths as small as 32 km as ared to SEASAT's 50 km resolution ability ks and Sailor, 1986; Born et al., 1987; Sailor .e Schack, 1987; Sandwell and McAdoo, in). This mission was designed to collect data proximately the same density and at the same ons as SEASAT (Born et al., 1987; Jenson Vooldridge, 1987).

of November, 1986, the Defense Mapping cy Aerospace Center (DMAAC), the agency nsible for editing and storing the GEOSAT had processed one third of the classified or 17.2 million data records (Van Hee, 1987). SAT's secondary mission is scheduled to con- in April, 1989, but the mission may continue he 1990's (Jenson and Wooldridge, 1987). GEOSAT data used to produce our map are on a preliminary analysis of the data in the rn oceans by Sandwell and McAdoo (in

ause the SEASAT mission was in operation the Austral winter, the results from high rly latitudes ($> 60°$) are very poor due to cts of sea ice. The GEOSAT mission, how- as collected data during the Austral summer. sult of the increased precision of the GEO- lata (around three times as precise as T), the information from high southerly s is exceptionally good (Sandwell and Mc- n press). For this reason, our interpretation onic features between 55° and 72° S is on GEOSAT altimetry data; all other features are based on SEASAT data.

on of the vertical and signal filtering

rder to emphasize the subtle variations in surface, the slope of the sea surface (de- of the vertical) was used to map the fabric of the ocean floor. The deflection ertical signal is the angle, in microradians, the line connecting the satellite and the ace, and the line normal to the sea surface.

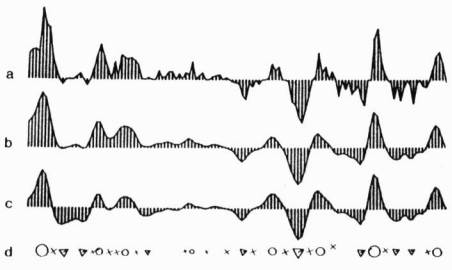

Fig. 3. The processing steps performed on the data. a. An unfiltered deflection of the vertical profile. b. A low-pass Gaussian filter removed wavelengths less than 19.8 km to decrease the short-wavelength noise. c. A high-pass Gaussian filter removed wavelengths greater than ~200 km. d. The positions of the peaks, troughs and zero crossings (inflection points) were recorded and represented by circles, triangles and crosses, respectively, which were scaled according to the amplitude of the signal. Only those peaks and troughs with amplitudes greater than the 7.5 μrad threshold were retained.

In essence, it is the first derivative of the sea surface. Taking the first derivative of the altimetry signal, however, tended to increase the short-wavelength noise (Fig. 3a).

To eliminate the short-wavelength noise, we convolved a Gaussian-shaped filter ($\exp[-t^2/2S^2]$; $S = 1$ s) with each profile. The satellite has a ground velocity of 6.6 km/s so this filter removes wavelengths less than 19.8 km (a distance equal to the spacing of three consecutive altimetry measurements). This resulted in a considerably smoother signal with well-defined peaks and troughs (Fig. 3b). After the short-wavelength noise was eliminated, the next step was to remove the broad, long-wavelength features of the geoid associated with deep-seated gravity anomalies and thermal convection. To remove the long-wavelength component of the signal, we used the same filter with a half-width of 10 s that eliminated features with wavelengths shorter than 200 km. The filtered profile was then subtracted from the original profile. The resulting band-pass filtered signal (Fig. 3c), though similar in shape to the previous one, is more symmetrically disposed about the baseline. In Fig. 4 the band-pass filtered deflection of the vertical profile is plotted along ascending satellite tracks in the Northeast Pacific;

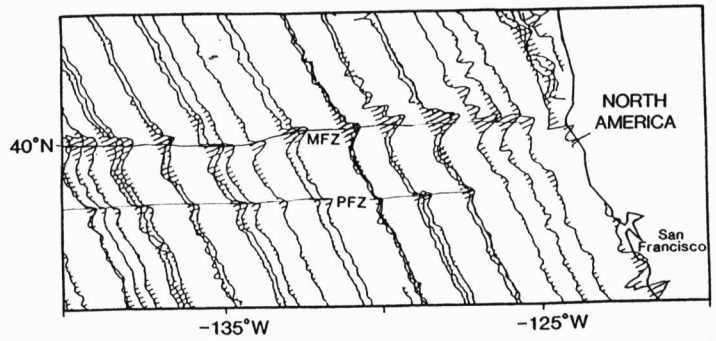

Fig. 4. The ascending, filtered deflection of the vertical profiles are plotted along the satellite tracks in the North Pacific. *MFZ*—Mendocino Fracture Zone; *PFZ*—Pioneer Fracture Zone (after Sandwell, 1984b).

the locations of the Mendocino and Pioneer fracture zones can be clearly seen.

Map preparation

In order to produce the tectonic fabric map (Fig. 1), the peaks and troughs of the deflection of the vertical signal were "picked", i.e., represented by discrete symbols (Fig. 3d). As illustrated in Fig. 3d, circles represent peaks (positive slopes in the sea surface), and triangles represent troughs (negative slopes in the sea surface). The symbols were scaled in proportion to the absolute magnitude of the amplitude of the signal (in microradians). The x's and plus signs represent the location where the signal crosses the zero line (inflection point). These symbols were then connected to form linear features (Fig. 5) As illustrated in this figure, this technique allowed us to plot data from both the ascending and descending satellite paths simultaneously, without crowding or confusion. Figure 6 illustrates the authorship responsibilities for the interpretations of the tectonic fabric (Fig. 1).

The satellite altimetry picks were generated by converting the amplitudes of the signals from meters/second to microradians. Not every peak and trough were picked, however. A threshold amplitude, representing the minimum amplitude for which a peak or trough would be "picked", was determined by trial and error. The value that we chose for the threshold amplitude (7.5 μrad) is slightly less than the amplitude of very short-wavelength noise as determined by Brammer and Sailor (1980).

The next step in the preparation of the tectonic fabric map was to plot the SEASAT picks on Mercator basemaps at a scale of 1 : 10,000,000. The picks for the ascending and descending tracks were plotted on separate sheets, and independent interpretations of the tectonic fabric were made for each sheet. For E–W trending features, the descending deflection of the vertical signal is opposite the ascending signal. Since the majority of tectonic features in the oceans are E–W trending, we compensated for this by switching the peak and trough symbols for the descending data set so

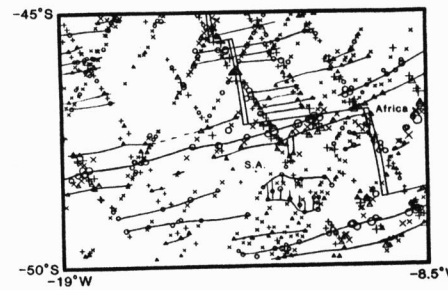

Fig. 5. A composite of the "picks" (see Fig. 3d for explanation) along the ascending and descending satellite tracks in the South Atlantic demonstrates how lineations for the tectonic fabric map were obtained by connecting like symbols. The ridge between the African and South American plates is from the Paleoceanographic Mapping Project (POMP) tectonic data compilation *S.A.*—South America.

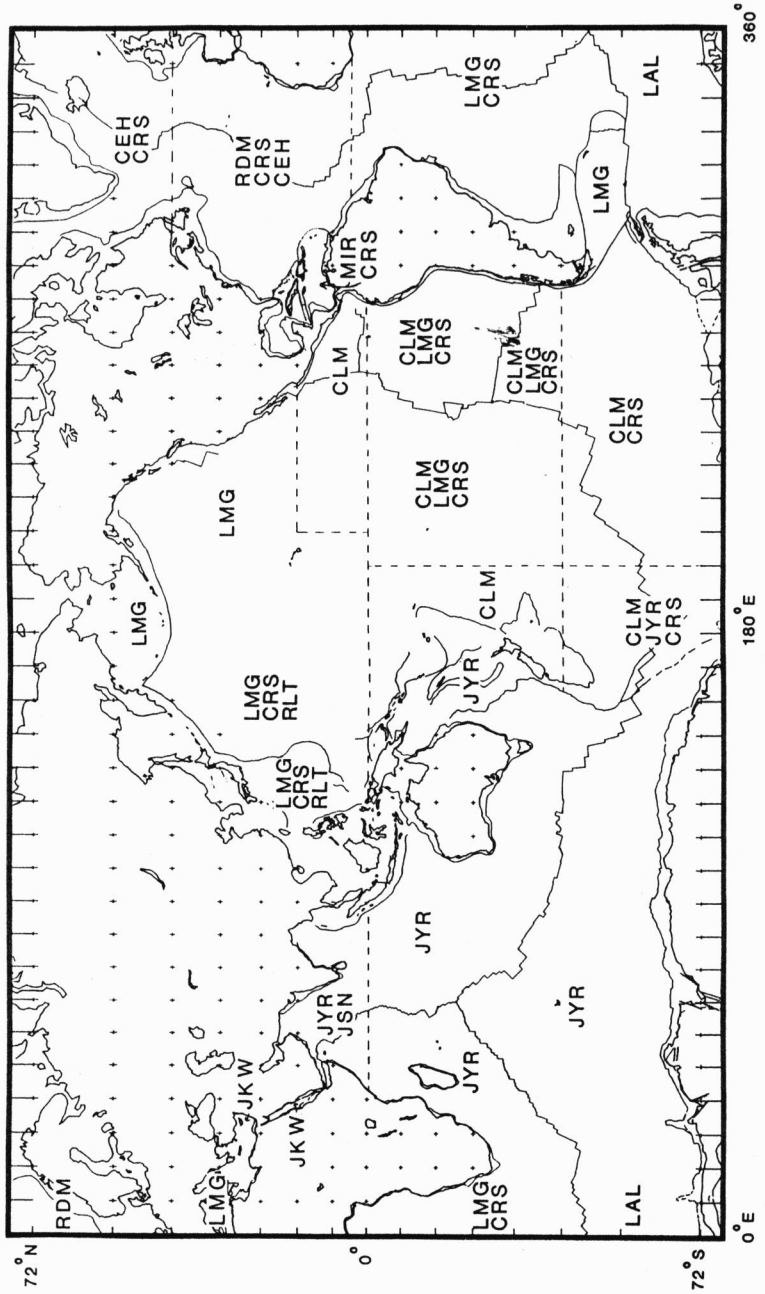

Fig. 6. Authorship responsibilities for the tectonic fabric map (Fig. 1). D.T. Sandwell and L.M. Gahagan processed the data.

as to obtain a consistent interpretation on both ascending and descending sheets (Gahagan, 1987). Typically, the interpretation of the tectonic fabric would begin with the identification of the major features. The identification of these features provided a framework from which more speculative interpretations could be made. After these preliminary interpretations were made, the interpretations from the ascending and descending sheets were superimposed and a final composite map was made (Fig. 1). By independently interpreting the tectonic fabric for the ascending and descending tracks, we could confidently differentiate between actual features and spurious interpretations. In this case, actual features would appear on both the ascending and descending maps, whereas spurious features were less consistent. In all cases, by combining the interpretations from the ascending and descending tracks we were able to draw more consistent and continuous features. The last stage in map interpretation was to compare the interpreted tectonic features with bathymetric data (GEBCO maps) in order to delete obvious errors and misinterpretations.

Discussion

Map interpretation: Reading the red and blue lines

A variety of tectonic features, including fracture zones, spreading axes, seamounts, aseismic plateaus and trenches, can be identified from the lineations illustrated in Fig. 1. In the following section we provide guidelines for identifying these tectonic features and delineating their boundaries. It has been our experience that when detailed comparisons of the tectonic fabric map and bathymetric maps are made, there is excellent agreement between the location of known features and our predictions from satellite altimetry.

We color-coded the lineations we obtained by connecting the picks, using blue for lines through peaks (circles) and red for lines through troughs (triangles). The red and blue lines can be regarded in a variety of ways. Essentially, they represent positive (blue) and negative (red) slopes of the sea surface. Because the slope in the sea surface is directly related to the horizontal component of the gravity field, the blue and red lines represent the positive (blue) and negative (red) horizontal gravity anomalies. As discussed earlier, the gravity anomalies are due primarily to the topography of the sea floor (fracture zones, trenches, etc.) and, as a consequence, the red and blue lines can also be thought of as lines along the maximum slopes of these submarine features. A blue line indicates an upslope direction, and, conversely, a red line means a downslope direction. For instance, in the case of a fracture zone, a red line indicates that the satellite crossed from younger crust over to older crust, going from high ground *down* to low ground, in accordance with the depth–age step.

The tectonic fabric on our map is not only constructed from red and blue lineations, but also from red and blue hatched zones. These zones are the result of broad, uneven or "rough" gravity surfaces that cause several peaks (or troughs) to occur together instead of one maximum peak (or trough) (Figs. 3c and d). The lines forming the hatching were drawn through one or more symbols and do not correspond to the number of symbols present. These broad zones of positive (blue) and negative (red) slope occur both over oceanic crust and over continental crust along the continental margins. These hatched zones may be due to (1) the expression of bathymetric features (e.g., the Rio Grande and Walvis ridges) or basement structures (e.g., the Colorado and Salado basins), (2) the presence of volcanism associated with hot spots or "leaky transforms," (3) areas of compression and extension along fracture zones, or (4) some deeper, unknown cause.

Because the blue and red lines represent slopes (gradients), there is one additional ambiguity: Which way is up? The slope is a vector that has both a magnitude and a direction. To interpret the map, one must read it from south to north. In this manner, a blue line indicates that the slope is increasing from south to north (upslope); conversely a red line indicates that the slope is decreasing from south to north (downslope). A ridge would have a blue line (upslope) along its southern edge, and a red line (downslope) along its northern edge. A trench or valley would have the opposite pattern, i.e., a red line (downslope) along its southern edge and a blue line (upslope) along

ıorthern edge. The meaning of the blue and lines can be best understood by referring to olors associated with the continental margins ig. 1. All S-facing continental margins are ed by blue lines (upslope), while all N-facing ins are marked by red lines (downslope). It be remembered that the blue and red lines ot correspond to the tectonic features, themes, but rather the colored lines indicate the mum slopes or gradients associated with these res.

ıe patterns of sea-surface slope associated major tectonic features are generally htforward; each tectonic feature has its own rn. In the following section, we review the ns in sea-surface slope associated with fracones, seamounts, ridges, aseismic plateaus, ıental margins and trenches.

ıcture zones

ıe long, linear features associated with fracones are the most distinctive features in Fig. owever, these tectonic flowlines, which have ded the movement of plates through time, do orrespond to the fracture zones on a one-to-asis. The location of the fracture zone relative to the red and blue lines depends on: (1) the morphology of the fracture zone, (2) the spreading rate of the adjacent ridge axis and (3) the age offset across the fracture zone. In general, fracture zones with small age offsets that were generated along ridges with slow spreading rates are characterized by deep valleys (Fig. 7aa). These fracture zones are characterized by a positive anomaly and a negative anomaly in the slope of the sea surface (Fig. 7a). In these cases, the fracture zone will lie between a pair of red and blue lines (Fig. 1). The red line that is always located to the south of the blue line, indicates the downslope section of the fracture zone valley; the blue line indicates the upslope section.

At the other end of the spectrum are those fracture zones such as the Mendocino Fracture Zone that are characterized by large age offsets and that are associated with fast-spreading ridges. Topographically, these fracture zones are characterized by large escarpments (Fig. 7b). The sea-surface slope can be positive (Fig. 7b) or negative depending on whether the crust is younger or older to the north of the fracture zone. Fracture zones with a large age offset in which the crust is younger to the north of the fracture zone will be marked by a blue line (upslope to the north). Fracture zones with large age offsets in which the crust is older to the north of the fracture zone will be marked by a red line (downslope to the north).

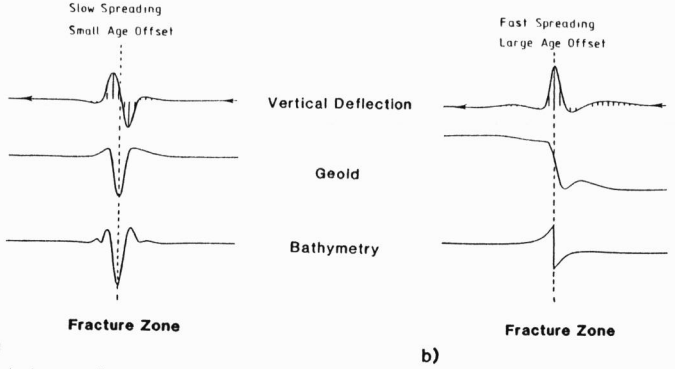

Within a particular spreading regime, fracture zones are characterized, to an extent, by particular bathymetric expressions that cted by the geoid. If the spreading rate and age offset along a fracture zone and the morphology of the fracture zone are the deflection of the vertical profile can be used to locate the fracture zone. a. A fracture zone associated with a slow g rate and a small age offset is characterized by a large trench and, as a result, is located at the inflection point of the n of the vertical profile. b. A fracture zone associated with a fast spreading rate and a large age offset is characterized by a arpment and, as a result, is located at the peak of the deflection of the vertical profile (as the satellite travels from older to younger crust).

These two end-member cases are based on the depth–age step associated with age differences and cooling of the oceanic crust. This depth–age step may be overprinted by other morphologies due to other tectonic processes such as horizontal thermal contraction and crustal warping (Collette, 1986). The gravity anomalies associated with the individual fracture zone morphology may cause additional lines of the color to be present, but in general, these lines will be subdued and less continuous.

Spreading ridges

As mentioned above, the symbol switching and the obliqueness with which many of the ridges intersected the satellite tracks made it difficult to identify spreading ridges. As a result, only parts of the Southwest, Central, and Southeast Indian ridges are recognizable on our map. The geoid signature of a ridge, like a fracture zone, depends on the spreading rate. A slow-spreading ridge, such as the Southwest Indian Ocean Ridge, usually possesses an axial trough which is reflected in the geoid signal. In passing over such a ridge, the satellite first measures an increase in slope, corresponding to a blue lineation on our map, due to the increase in height of the ridge. The maximum downward slope of the axial trough is represented by a red line and the maximum upward slope of the other side of the axial trough is represented by a blue line. As the satellite continues over the other side of the ridge, the maximum downward slope of the ridge is represented by a red line. The location of the axial trough is actually between the first red line and the second blue line. This ideal representation is best seen along the Southwest Indian Ridge between the Indomed and Gallieni fracture zones (numbers 24 and 25 in Fig. 8).

Seamounts

The seamounts and major island archipelagos are illustrated on the map by small circles and irregular, circular areas (Fig. 1). The deflection of the vertical signal for a seamount reflects (1) the positive slope in the sea surface measured by the satellite as it approached the seamount from the southeast and (2) the negative slope as it continued over the other side of the seamount. Therefore, on our map, the southern half of the seamount is marked by a blue line (positive slope), and the northern half is marked by a red line (negative slope).

If the satellite passed directly over the seamount, then the actual location of it would be at the inflection point, or zero crossing, of the signal. The satellite does not, however, need to pass directly over the seamount to register the associated gravity anomaly. As a result, the circles on our map do not represent the exact location of a seamount but merely indicate the presence of one in the area. The size of the circles is based on the size of the amplitude of the signal and does not correspond to the size of the seamount since the amplitude of the signal depends not only on the size of the seamount but also on the degree of compensation and the distance of the seamount from the satellite track (Craig and Sandwell, in press). Because of the minimum threshold we set in our processing to remove short-wavelength noise, the minimum amplitude of a signal that was recognized in our study as a seamount was 7.5 μrad or 7.5 mGal of horizontal gravity component.

The similarity of the deflection of the vertical signal over a seamount and across a linear feature, such as a fracture zone, can make recognition of a seamount a difficult task, except in cases where several tracks, crossing over the same seamount, clearly define the outline of the structure. One method used to determine which type of feature a signal represented was to examine the extent of a signal. If the signal for a feature extended over a large ($>$ 100 km) area across several tracks, then the signal was probably due to a more elongate feature instead of a seamount since the signal of an isolated seamount rarely extends more than 100 km (Craig and Sandwell, in press). Another method used to identify seamounts was to visually compare the amplitude of the suspected seamount signal with other signals in the area. If the amplitude of the signal was visually larger, it was interpreted as a seamount. Using these criteria, we

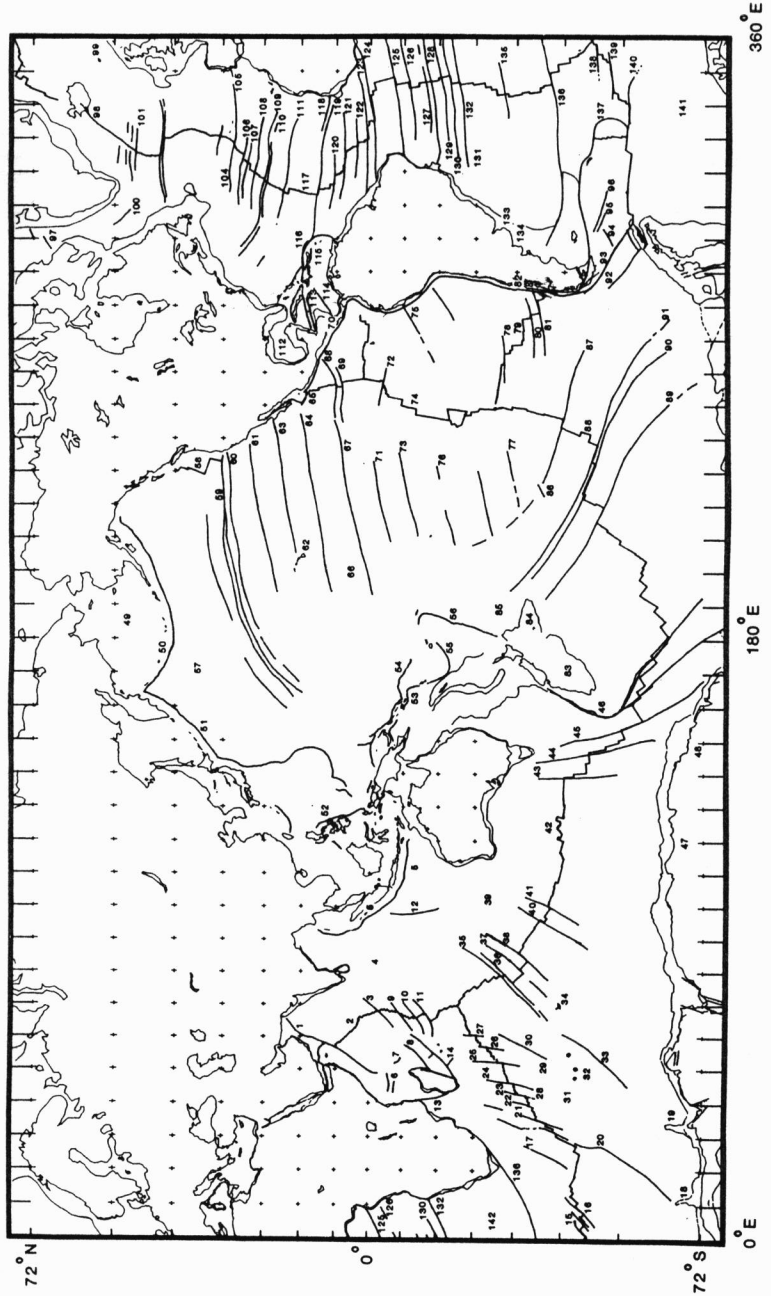

were able to recognize the major seamounts as well as identify suspected seamounts.

Trenches

Our map depicts the deep ocean trenches, which are located near continental margins and island arcs, as linear features. The height of the sea surface increases in response to the slight upwarping of the subducting plate, resulting in a peak in the deflection of the vertical signal. On our map, this feature is colored blue since it has a positive slope. Depending on the magnitude of upwarping, this feature may be represented on our map as either a single line or a broad linear hatched zone parallel to the trench. The maximum downward slope of the sea surface over the outer trench is represented by a red line on our map. The inflection point, or zero crossing, of the deflection of the vertical signal marks the location of the trench axis. Over the inner trench slope, the height of the sea surface increases. The resulting positive slope of the sea surface corresponds to a blue line or a broad zone on our map.

Due to the N–S trajectory of the satellite tracks, features that are oriented E–W are more clearly defined than features oriented N–S. This bias is particularly evident with regard to the trenches. Parts of the Peru–Chile Trench are not well defined. In contrast, areas of the Mid-American, Aleutian and Kurile trenches are clearly delineated.

Continental margins and aseismic plateaus

For our purposes, the term continental margin refers to the steepest bathymetric gradient around a continent (the shelf–slope break). An aseismic plateau refers to a submarine feature, other than the mid-ocean ridges, which may be of either continental or oceanic origin. The map presented in this study reveals information on both the outline and the apparent structure along continental margins and on aseismic plateaus.

As the satellite, travelling northwards, crosses over the continental margin from oceanic crust to continental crust, the height of the sea surface increases. This results in a peak in the deflection

Fig. 8. Areas mentioned in the text as well as features that are visible on the tectonic fabric map are shown here.
Indian Ocean: *1*—Owen Fracture Zone (FZ); *2*—Carlsberg Ridge; *3*—Mabahiss FZ; *4*—Central Indian basin; *5*—Java–Sumatra Trench (TR); *6*—Somali Basin; *7*—Amirante TR; *8*—Mahanoro and Mauritius FZ; *9*—Vema FZ; *10*—Argo FZ; *11*—Marie Celeste FZ; *12*—Investigator FZ; *13*—Davie Ridge; *14*—Mascarene Basin; *15*—Bouvet, Moshesh and Isla Orcadas FZ; *16*—Shaka and Dingaan FZ; *17*—Dutoit FZ; *18*—Astrid Ridge; *19*—Gunnerus Ridge; *20*—Astrid FZ; *21*—Prince Edward FZ; *22*—Bain FZ; *23*—Discovery FZ; *24*—Indomed FZ; *25*—Gallieni FZ; *26*—Atlantis II FZ; *27*—Melville FZ; *28*—Del Caño Rise; *29*—Crozet Bank; *30*—L'Astrolabe FZ; *31*—Conrad Rise; *32*—Marie Dufresne Seamount; *33*—Kerguelen FZ; *34*—Kerguelen Plateau; *35*—Amsterdam FZ; *36*—St. Paul FZ; *37*—Mitra FZ; *38*—Varuna Fz; *39*—Broken Ridge Plateau; *40*—Soma FZ; *41*—Surya FZ; *42*—Australian–Antarctic Discordance; *43*—George V FZ; *44*—Tasman FZ; *45*—Balleny FZ; *46*—Macquarie Ridge; *47*—Wilkes Land; *48*—George V Land.
Pacific Ocean: *49*—Bering Sea; *50*—Aleutian TR; *51*—Kuril TR; *52*—Philippine TR; *53*—South Solomon TR; *54*—Vitiaz TR; *55*—New Hebrides TR; *56*—Tonga–Kermadec TR; *57*—Emperor Seamounts; *58*—Juan de Fuca Ridge; *59*—Mendocino FZ; *60*—Pioneer FZ; *61*—Murray FZ; *62*—Hawaiian Islands; *63*—Molokai FZ; *64*—Clarion FZ; *65*—Rivera FZ; *66*—Line Islands; *67*—Clipperton FZ; *68*—Tehuantepec FZ; *69*—Siquieros FZ; *70*—Mid-American TR; *71*—Galapagos FZ; *72*—Quebrado FZ; *73*—Marquesas FZ; *74*—East Pacific Rise; *75*—Mendana FZ; *76*—Austral FZ; *77*—Agassiz FZ; *78*—Chile FZ; *79*—Chile Rise; *80*—Valdivia FZ; Guafo FZ; *82*—Peru–Chile TR; *83*—Cambell Plateau; *84*—Chatham Rise; *85*—Louisville Ridge; *86*—Henry Trough; *87*—Menard FZ; *88*—Pacific–Antarctic Ridge; *89*—Udintsev FZ; *90*—Tharp FZ; *91*—Heezen FZ; *92*—Hero FZ; *93*—Shackleton FZ; *94*—West Scotia Ridge; *95*—Quest FZ; *96*—Endurance FZ.
Atlantic Ocean: *97*—Baffin Bay; *98*—Reykjanes Ridge; *99*—Faeros Ridge; *100*—Labrador Sea; *101*—Bight FZ; *102*—Charlie Gibbs FZ; *103*—Kurchatov FZ; *104*—Pico FZ; *105*—East Azores FZ; *106*—Ocanographer FZ; *107*—Hayes FZ; *108*—Cruiser FZ; *109*—Atlantis FZ; *110*—Tyro FZ; *111*—Kane FZ; *112*—Gulf of Mexico; *113*—Cayman Trough; *114*—Hess Escarpment; *115*—Muertos Trough; *116*—Puerto Rico TR; *117*—Atlantic Ridge; *118*—Jacksonville FZ; *119*—Fifteen-Twenty FZ; *120*—Vema FZ; *121*—Sierra Leone FZ; *122*—Four North FZ; *123*—St. Paul FZ; *124*—Romanche FZ; *125*—Ascension FZ; *126*—Bode Verde FZ; *127*—St. Helene; *128*—Hotspur FZ; *129*—Martin Vaz FZ; *130*—Rio de Janeiro FZ; *131*—Rio Grande Ridge; *132*—Rio Grande FZ; *133*—Salado Basin; *134*—Colorado Basin; *135*—Tristan da Cunha FZ; *136*—Falkland–Agulhas FZ; *137*—South Sandwich TR; *138*—Conrad FZ; *139*—Bullard FZ; *140*—South Sandwich FZ; *141*—Weddell Sea; *142*—Walvis Ridge.

of the vertical signal corresponding to the point of maximum positive slope. Going from continental crust to oceanic crust, the height of the sea surface decreases, resulting in a corresponding trough in the deflection of the vertical signal. Therefore, as mentioned above, all S-facing continental margins (e.g., south of Australia) are marked on our map by blue lines (positive slope), while all N-facing margins (e.g., northwest of the U.K.) are marked by red lines (negative slope).

The outlines of continental margins and aseismic plateaus are often overprinted, however, by broad zones of blue and red hatching. As mentioned above, these zones may be due to a number of causes. The pattern of these zones along the continental margins suggests that they may reveal basement structures that are buried beneath the sedimentary cover.

Identification of major tectonic features on the fabric map

The primary goal of this study has been the identification of tectonic features from satellite altimetry data. In this section we compare the features that are present on the tectonic fabric map (Fig. 1) with known tectonic and bathymetric features. We also discuss how the extent or shape of these features must be modified in the light of satellite altimetry data, and describe new tectonic features that were previously unmapped. Figure 8 illustrates the location of the areas and major tectonic features discussed in this section, identified by number. The corresponding numbers will be displayed in brackets ([ ]) after the feature or area.

Atlantic Ocean

Because the N–S trend of the satellite tracks enhance E–W trending features, the fracture zones in the Atlantic Region are clearly visible (Fig. 1). These include the Charlie Gibbs [102], Kurchatov [103], Pico [104], East Azores [105], Oceanographer [106], Hayes [107], Cruiser [108], Atlantis [109], Tyro [110], Kane [111], Jacksonville [118] and Fifteen-Twenty [119] fracture zones in the central Atlantic, and the Vema [120], Sierra Leone [121], Four North [122], St. Paul [123], Romanche [124], Ascension [125], Bode Verde [126], St. Helene [127], Hotspur [128], Martin Vaz [129], Rio de Janeiro [130], Rio Grande [132], Tristan da Cunha [135] and the Falkland–Agulhas [136] fracture zones in the South Atlantic. In many cases, the trend of the fracture zone can be extended closer to the continental margins (e.g., Charlie Gibbs [102], Azores [105], Atlantis [109], Kane [111], St. Paul [123], Romanche [124] and Ascension [125] fracture zones). The trend of the Romanche and Ascension fracture zones can be traced up onto the continental margins of Africa and South America. In cases where there is a large age offset across a fracture zone, the colors may change across the ridge (e.g. the Falkland–Agulhas Fracture Zone [136]). As the satellite crosses from younger to older crust on one side of the ridge, the bathymetry and sea surface decrease in height, corresponding to a red line on the map. As the satellite crosses from older to younger crust on the other side of the ridge, the bathymetry and sea surface increase in height, corresponding to a blue line. This color change on the map can be used to determine the location of the ridge. On the tectonic fabric map in the North Atlantic, numerous, short, unnamed fracture zones parallel the Bight Fracture Zone [101] (Fig. 1). In Baffin Bay [97], there are several pairs of NE–SW trending lineations that may represent fracture zones.

Except for Reykjanes Ridge [98], which is delineated by a parallel series of NE–SW trending hatched zones, the spreading ridges in the Atlantic region are difficult to identify. However, in some cases the transition across the ridge axis can be seen by a change in the slope of the sea surface, i.e., a change in the color of the lineations from red to blue (e.g. the Falkland–Agulhas Fracture Zone). Lineations in the center of the Labrador Sea [100] probably represent a spreading axis that became extinct in the Early Tertiary (Srivastava and Tapscott, 1986).

In addition to the steep gradients in the sea surface identified by the red and blue lineations, there are gentle slopes in the sea surface identified by broad zones of blue and red hatching. These broad zones are visible in the Barents Sea, on the Reykjanes Ridge [98], and along the continental margins. One of the most dramatic examples of this kind of pattern occurs along the margin of southeastern Argentina and the Falkland Plateau (Fig. 1). In this area the red and blue hatching probably represents basement structures that are buried beneath a thin veneer of sediments (e.g., Salado [133] and Colorado [134] basins). These zones of red and blue also extend into the ocean basins where they usually correspond to volcanic edifices and aseismic plateaus (Rio Grande [131]–Walvis Ridge [142] and Faeroes Ridge [99]).

The complex pattern of the tectonic fabric in the Caribbean and Gulf of Mexico [112] region is due to a variety of tectonic features. The lineations that are parallel to the margins of the Gulf of Mexico represent stretched continental crust, as well as a narrow zone of oceanic crust that lies in the center of the gulf (Buffler and Sawyer, 1983). The Cayman Trough [113] and Hess Escarpment [114] are well defined by sets of parallel lineations. The Muertos Trough [115], south of Hispaniola, and the Puerto Rico Trench [116] are outlined by broad swells in the slope of the sea surface (Fig. 1).

Indian Ocean

Unlike the tectonic fabric of the Atlantic which is dominated by fracture-zone trends, the tectonic fabric of the Indian Ocean reveals a variety of tectonic features. These features include young and old fracture zones, active and extinct spreading centers, volcanic features, aseismic plateaus, rifted continental margins and trenches.

The fracture zone lineations in the Indian Ocean are generally more difficult to identify due to their primarily N–S orientation. However, distinct fracture-zone trends can be recognized in the vicinity of slow-spreading ridges. Along the Central Indian Ridge, the Owen [1], Mabahiss [3], Vema [9], Argo [10] and Marie Celeste [11] fracture zones can be identified. Along the Southwest Indian Ridge, the Melville [27], Atlantis II [26], Gallieni [25], Indomed [24], Discovery [23], Prince Edward [21], Bain [22] and Dutoit [17] fracture zones are recognizable. The L'Astrolabe Fracture Zone [30] to the south of the Southwest Indian Ridge is also visible. Although located in a faster spreading regime, several fracture zones along the Southeast Indian Ridge can be identified: the Amsterdam [35], St. Paul [36], Mitra [37], Varuna [38], Soma [40] and Surya [41] fracture zones (McKenzie and Sclater, 1971). Using satellite altimetry data, the trends of several fracture zones can be extended closer to the continental margins (e.g., the George V [43], Tasman [44] and Balleny [45] fracture zones). Older fracture zones, such as the Davie Ridge [13] in the Somali Basin [6] and the Mauritius and Mahanoro fracture zones [8] south of the Mascarene Basin [14] are visible on the tectonic fabric map (Fig. 1). The bends in the red and blue lineations corresponding to the Astrid [18] and Investigator [12] fracture zones reveal major changes in spreading direction.

Parts of the Central, Southwest and Southeast Indian ridges, due to their E–W orientation, can be identified on the tectonic fabric map. The most easily identified ridge segments are located along the southeastern area of the Carlsberg Ridge [2], along the Southeast Indian Ridge south of the Agulhas Basin, between the Indomed Fracture Zone [24] and Central Indian Triple Junction, and along the Australian–Antarctic Discordance [42]. The extinct spreading center in the Mascarene Basin [14] and south of Réunion Island is outlined by two pairs of NW–SE trending red and blue lineations (Schlich, 1982).

As in the Atlantic region, the blue and red hatched zones represent broad, gently sloping areas of the sea surface. In the Indian Ocean, the most prominent of these features correspond to the Kerguelen [34] and Broken Ridge [39] plateaus (Fig. 1). Using the satellite altimetry data, the extent of the Kerguelen Plateau has been mapped in detail, and a variety of associated features, such as the Labuan Basin and Elan Bank, have been identified (Coffin et al., 1986). Other features, such as the Del Caño Rise [28], Crozet Bank [29] and the Conrad Rise [31], are clearly visible on the fabric map and new seamounts have been identified northeast of Marion Dufresne Seamount [32]. Although the Ninetyeast Ridge and the Chagos–Laccadive Ridge are major tectonic features, they do not appear on our tectonic fabric map because of their orientation.

The continental margins of Antarctica (Wilkes Land [47]) and southern Australia display hatched zones that may correspond to broad areas of

retched continental or transitional crust or arginal sedimentary basins. Similar hatched areas ong the eastern margin of India and south of kistan may be related to the progradation of anges and Indus fans. Of particular interest is e set of E–W trending hatched zones in the ntral Indian Basin [4]. These features represent e buckling and folding of oceanic crust related the ongoing collision of India and Eurasia Veissel et al., 1980; McAdoo and Sandwell, 1985). The Java–Sumatra [5] trenches are illustrated the tectonic fabric map by a series of arcuate eations. Similar lineations are observed along Seychelle Islands south of the Amirante Trench

Pacific Ocean

The tectonic fabric of the West and Central cific is dominated by irregular or circular fea- es representing seamounts. Several subparallel mount trends can be recognized. The most minent are associated with the Hawaiian Emperor [57] archipelago, the Line Islands], the Austral Islands, Easter Island and the uisville Ridge [85] (Craig and Sandwell, in ss).

In contrast, the most prominent tectonic fabrics the East Pacific Basin are the satellite altimetry ations associated with fracture zones. In the rtheast Pacific, tectonic lineations associated h the Mendocino [59], Pioneer [60], Murray], Molokai [63], Clarion [64], Rivera [65], pperton [67], Tehuantepec [68] and Siquieros fracture zones are clearly visible. Our inter- tation of the satellite altimetry data suggests the Mendocino Fracture Zone [59] can be nded west of the Emperor Islands [57], the rray [61] and Molokai [63] fracture zones can xtended to the Hawaiian Islands [62], and the pperton Fracture Zone [67] may extend west of Line Islands [66] (Fig. 1). In the Southeast and thwest Pacific, the Galapagos [71], Marquesas Quebrada [72], Mendana [75], Chile [78], divia [80], Guafo [80], Austral [76], Agassiz Menard [87], Heezen [91], Tharp [90], Udint- [89] and Hero [92] fracture zones can be ntified on the tectonic fabric map (Fig. 1). The rquesas [73], Austral [76] and Guafo [80] fracture zones in particular can be mapped in greater detail than is available from bathymetric maps. In the Southwest Pacific, numerous fracture zone lineations have been identified that lie parallel to the major fracture zones (the Heezen [91], Tharp [90] and Udintsev [89] fracture zones). In most cases, the trends of these fracture zones can be extended nearly to the margin of Antarctica.

Due to its low relief and predominantly N–S orientation, the East Pacific Rise [74] is not visible on the tectonic fabric map. Similarly, the Juan de Fuca Ridge [58], Chile Rise [79] and the Pacific–Antarctic Ridge [88] cannot be mapped directly. The locations of these spreading centers, however, can often be inferred by noting the change in the slope of the sea surface along fracture zones near the ridge axes. Further, the ridges can be located by observing where the lineation changes from red to blue (e.g., along Udintsev Fracture Zone [89] at 55°S, 145°W).

Another rift-related feature, the Henry Trough [86] (45°S, 135°W), is clearly visible on the tectonic fabric map (Fig. 1). The L-shaped bend south of the Menard Fracture Zone [87] marks the location where a propagating ridge rifted older oceanic crust (Cande et al., 1982). The satellite-derived lineations are well defined in this region due to the contrasting ages of the oceanic crust (60 Ma compared to 47 Ma).

As expected, the trenches are best expressed where the satellite tracks cross them at a high angle (the Aleutian [50], Kurile [51], South Solomon [53], Vitiaz [54], New Hebrides [55] and Mid-American [70] trenches). The expression of a trench is more subdued where the satellite tracks run subparallel to the axis (the Philippine [52], Tonga–Kermadec [56] and Peru–Chile [82] trenches). The trench axis is marked by a single red line. Along some trenches (the Aleutian [50], Kurile [51] and New Hebrides [55]), a broad positive anomaly in the slope of the sea surface is present seaward of the trench (blue hatching). This anomaly is probably due to the bending and upwarping of the subducting oceanic lithosphere.

Other broad areas of hatching indicating gentle slopes of the sea surface are present in the Pacific. The hatching over the Campbell Plateau [83] and Chatham Rise [84] (New Zealand) is similar to the tectonic fabric over the Falkland Plateau, and probably represents basement structures associated with stretched continental or transitional crust. Similar features are observed in the Bering Basin [49] and along the Bering shelf margin.

Circum-Antarctic region

As discussed in the introduction, because the SEASAT mission was in operation during the Austral winter, the results from high southerly latitudes (> 60°) were adversely affected by the effects of sea ice. The GEOSAT mission, however, collected data during the Austral summer; as a result, the information from high southerly latitudes is exceptionally good. Numerous new tectonic features can be identified using the GEOSAT data (Sandwell and McAdoo, in press). These features provide important constraints on the development of the Antarctic margin (Lawver et al., in press) and on the evolution of the southern oceans.

In the South Atlantic, the distinct fracture zone pattern surrounding the Bouvet Triple Junction is clearly visible (Fig. 1). Of particular interest is the fracture-zone pattern associated with the American–Antarctic Ridge (Barker and Lawver, 1988). The NW–SE trend of this fabric extends southward into the Weddell Sea [141], and ultimately to the continental margin of Antarctica.

East of the Weddell Sea, the tectonic fabric changes abruptly. A new set of NE–SW trending fracture zones intersects the Weddell Sea Fracture Zone lineaments. The most continuous lineament, the Astrid Fracture Zone [20], can be traced northward from the Astrid Ridge [18], across the Southwest Indian Ridge and towards the Mozambique Escarpment. This lineament is a flowline that records the relative movement of Africa with respect to Antarctica since the Late Jurassic (Bergh, 1987).

Another lineament is observed east of the Gunnerus Ridge [19], to the southwest of the Kerguelen Plateau [34]. This lineament, the Kerguelen Fracture Zone [33], is the flowline that records the relative movement of India with respect to Antarctica since the Early Cretaceous (Royer and Sandwell, in prep). It forms the western boundary of the Kerguelen Plateau [34]. The conjugate section of the Kerguelen Fracture Zone [33] on the Indian plate is difficult to identify; however, the matching fracture zone probably lies to the west of the Ninetyeast Ridge.

A third set of lineaments has been mapped between Australia and Antarctica. The most prominent fracture zone lineations in this set (George V [43], Tasman [44] and Balleny [45] fracture zones) run from southeast Australia to George V Land [48], Antarctica. These fracture zone lineations are flowlines that record the relative movement of Australia and Antarctica since the Late Cretaceous (Weissel and Hayes, 1972; Cande and Mutter, 1982). The broad zones of blue and red hatching along the coast of George V Land [48] and the south coast of Australia probably represent stretched continental or transitional crust formed during the earliest phases of rifting.

East of the Balleny Fracture Zone [45], the Macquarie Ridge [46] can be easily identified by a set of arcuate lineations. Further to the east, in the Southwest Pacific Basin, a dense NW–SE trending fracture zone fabric has been mapped. These fracture-zone trends are parallel to the Udintsev [89], Tharp [90] and Heezen [91] fracture zones, and extend the known limit of these fracture zones to higher latitudes. The southward extension of the Udintsev Fracture Zone [89] intersects the margin of western Antarctica at Pine Island Bay, between Thurston Island and Marie Byrdland (Sandwell and McAdoo, in press).

In the Scotia Sea, the Shackleton [93], Quest [95] and Endurance [96] fracture zones have been identified. Although the present-day spreading center is not recognized, the West Scotia Ridge [94], an extinct NE–SW trending ridge, can be seen on the fabric map (Fig. 1) (Barker and Burrell, 1977).

Summary and conclusions

Although most of the tectonic features cited above have been previously identified or suspected from ship-track data, the satellite altimetry data enhance our knowledge of them. The tectonic fabric map provides a greater resolution of the outline of many of these features while also permitting the extension of the physical limits of

aith features beyond what bathymetric charts w. This new information will no doubt play a t in various aspects of plate tectonic modelling; articular, the detail and extension of fracture e lineations, which have recorded plate move- it through time, may serve as additional con- ints for plate movement reconstruction.

Besides providing more detail on known fea- s, the tectonic fabric map also displays fea- s that are not apparent on global bathymetric s (GEBCO). The satellite data reveal the pres- of numerous seamounts in the North and tral Pacific and the distinct lack of seamounts he southern oceans (Craig and Sandwell, in s). As mentioned above, the extinct spreading er in the Mascarene Basin and parts of the theast Indian Ridge at the Australian–Antarc- Discordance are visible on the map.

Due to the lack of ship-track data in the south- oceans, the satellite data reveal several pieces information on fracture zone lineations and ds which are not seen on bathymetric charts. instance, between the major fracture zone itions in the Southwest Pacific Ocean are many ller lineations that may correspond to minor hartered fracture zones. In the Weddell Sea, trend of the lineations on the tectonic fabric reveals the spreading history of the area.

he tectonic fabric map also displays features are the result of the expression of deep-seated ity anomalies. These broad geoid anomalies ally define several aseismic plateaus such as Kerguelen, Broken Ridge and Campbell aus. The anomalies are visible over the con- ital crust of the Falkland Plateau as well as the oceanic crust slightly to the north of the au. In the Central Indian Ocean, these grav- nomalies appear as wrinkles on the tectonic e map (Weissel et al., 1980; Haxby, 1987; doo and Sandwell, 1985).

rom our analysis of SEASAT and GEOSAT lite altimetry data we have been able to map tectonic fabric of the ocean basins and con- ital margins. Using the slope of the sea surface lection of the vertical) we have identified frac- zones, spreading ridges, subducting trenches, ounts, aseismic plateaus and deeply buried features along the continental margins. The global uniformity of the spacing of the satellite data allows us to map known features in greater detail and in a more continuous manner, particularly in the southern oceans. The data have given us proof of the continuity of tectonic features that were previously shown by irregularly spaced ship-track data or magnetic anomaly offsets, as in the case of the southwestern extent of the L'Astrolabe Fracture Zone [30]. In addition to being able to identify known tectonic features, we have also identified numerous new tectonic elements. However, we have just barely scratched the surface and there is no doubt that in the future a wealth of additional information will be revealed by detailed studies of satellite altimetry data. The tectonic fabric map that we present in this paper is a starting point. The tectonic features that we have mapped will be used to (1) produce more accurate plate tectonic reconstructions, (2) identify epochs of global plate reorganization and (3) understand the subtle dynamics of the plate tectonic process.

The accuracy of plate tectonic reconstructions depends on the amount and quality of data that constrain the fit. The tectonic fabric we have mapped provides numerous additional control points and constraints for high-resolution plate tectonic reconstructions. We believe that the fabric itself has a story to tell. The tectonic fabric records the subtle changes in spreading direction through time. The "bumps" and "undulations" in the fabric flowlines reflect changes in plate motion. In future studies we hope to correlate these bumps and undulations between ocean basins in order to determine if these changes in plate motion were globally synchronous. Finally, as more satellite altimetry data become available, we hope to produce higher resolution tectonic fabric maps. These maps will be an essential tool for understanding the pattern of plate tectonic processes in time and space. From these maps we may be able to answer some of the following questions. "How often do ridge jumps occur?", "how do ridge segments change through time?", "do oceanic fracture zones extend onto the continental margins?", and, "are plate tectonic processes continuous or episodic?"

Acknowledgements

This work was supported by funding from Amoco International Oil Co., Chevron Overseas Petroleum Co., Conoco, Elf Aquitaine, Exxon Production Research, Mobil Oil Co., Petro-Canada, Phillips Petroleum, Shell Development Co. and Standard Oil Co. as part of their sponsorship of the Paleoceanographic Mapping Project at the University of Texas at Austin. This work was also partially supported by the NASA Geodynamics Program (NAG5-787). The Geology Foundation at the University of Texas at Austin is gratefully acknowledged. The digital database and maps at a scale of 1:10,000,000 for both the satellite altimetry picks and the interpreted tectonic fabric will be available in mid-1989. If you are interested, please write to the authors at address 3 at the beginning of this paper.

References

Barker, P.F. and Burrell, J., 1977. The opening of Drake Passage. Mar. Geol., 25: 15–34.

Barker, P.F. and Lawver, L.A., 1988. The Cenozoic evolution of the South American–Antarctic Ridge. Geophys. J., 94(3).

Bergh, H.W., 1987. Mesozoic seafloor off Dronning Maud Land, Antarctica. Nature, 269: 687.

Born, G.H., Mitchell, J.L. and Heyler, G.A., 1987. Design of the GEOSAT Exact Repeat Mission. John Hopkins Appl. Phys. Lab. Tech. Dig., 8: 260–266.

Brammer, R.F. and Sailor, R.V., 1980. Preliminary estimates of the resolution capability of the SEASAT radar altimeter. Geophys. Res. Lett., 7: 193–196.

Buffler, R.T. and Sawyer, D.S., 1983. Distribution of crust and early history, Gulf of Mexico basin. Gulf Coast Assoc. Geol. Soc. Trans., 35: 334–344.

Cande, S.C. and Mutter, J.C., 1982. A revised identification of the oldest sea-floor spreading anomalies between Australia and Antarctica. Earth Planet. Sci. Lett., 58: 151–160.

Cande, S.C., Herron, E.M. and Hall, B.R., 1982. The early Cenozoic tectonic history of the southeast Pacific. Earth Planet. Sci. Lett., 57: 63–74.

Cande, S.C., LaBrecque, J.L. and Haxby, W.B., in press. Plate kinematics of the South Atlantic: chron 34 to present. J. Geophys. Res.

Coffin, M.F., Davies, H.L. and Haxby, W.F., 1986. Structure of the Kerguelen plateau province from SEASAT altimetry and seismic reflection data. Nature, 324: 134–136.

Collette, B.J., 1986. Fracture zones in the North Atlantic: morphology and a model. J. Geol. Soc. London 143: 763–774.

Craig, C.H. and Sandwell, D.T., in press. The global distribution of seamounts from SEASAT profiles. J. Geophys. Res.

Gahagan, L.M., 1988. The mapping of tectonic features in the ocean basins from satellite altimetry data. Master's Thesis, Univ. Texas at Austin, Austin, 95 pp. (Unpubl.)

Hancock, D.W., Forsythe, R.G. and Lorell, J., 1980. SEASAT altimeter sensor file algorithms. I.E.E.E. Oceanic Eng., OE 5(2), pp. 93–99.

Haxby, W.F., 1987. Map of the gravity field of the world's oceans. Natl. Oceanic Atmos. Adm. Rep. MGG-3.

Haxby, W.F., Karner, G.D., LaBreque, J.L. and Weissel, J.K., 1983. Digital images of combined oceanic and continental data sets and their use in tectonic studies. Eos, Trans. Am. Geophys. Union, 64: 995–1004.

Jenson, J.J. and Wooldridge. F.R., 1987. The Navy GEOSAT mission: an introduction. John Hopkins Appl. Phys. Lab. Tech. Dig., 8: 169.

Lame, D.B. and Born, G.H., 1982. SEASAT measurement system evaluation: achievements and limitations. J. Geophys. Res., 87: 3175–3178.

Lawver, L.A., Royer, J.Y., Sandwell, D.T. and Scotese, C.R., in press. Evolution of the Antarctic continental margins. Int. Antarct. Earth Sci. Symp., 5th (Cambridge, U.K.).

Lorell, J., 1980. Algorithm development facility altimeter sensor algorithm specifications. Jet Propul. Lab. Intern. Rep. 622–2071, Revi. a.

MacArthur, J.L., Marth Jr., P.C. and Wall, J.G., 1987. The GEOSAT radar altimeter. John Hopkins Appl. Phys. Lab. Tech. Dig., 8: 176–181.

Marks, K.M. and Sailor, R.V., 1986. Comparison of GEOS-3 and SEASAT altimeter resolution capabilities. Geophys. Res. Lett., 13: 697–700.

McAdoo, D.C., 1981. Geoid anomalies in the vicinity of subduction zones. J. Geophys. Res., 86: 6073–6090.

McAdoo, D.C. and Sandwell, D.T., 1985. Folding of oceanic lithosphere. J. Geophys. Res., 90: 8563–8569.

McConathy, D.R. and Kilgus, C.C., 1987. The Navy GEOSAT mission: an overview. John Hopkins Appl. Phys. Lab. Tech. Dig., 8: 170–175.

McKenzie, D. and Sclater, J.G., 1971. The evolution of the Indian Ocean since the Late Cretaceous. Geophys. J.R. Astron. Soc., 25: 437–528.

Mitchell, J.L., Hallock, Z.R. and Thompson, J.D., 1987. REX and GEOSAT: progress in the first year. John Hopkins Appl. Phys. Lab. Tech. Dig., 8: 234–244.

Parke, M.E., Born, G.H. and Scott, J.F., 1980. SEASAT altimeter geophysical algorithm specifications. Jet Propul. Lab. Intern. Rep. 622–226.

Royer, J.Y. and Sandwell, D.T., in prep. Evolution of the Eastern Indian Ocean since the Late Cretaceous: constraints from GEOSAT altimetry.

Sailor, R.V. and LeSchack, A.R., 1987. Preliminary determination of the GEOSAT radar altimeter noise spectrum. John Hopkins Appl. Phys. Lab. Tech. Dig., 8: 182–183.

. R.V. and Okal, E.A., 1983. Applications of SEASAT imeter data in seismotectonic studies of the South-Central cific. J. Geophys. Res., 88: 1572–1580.
ell, D.T., 1984a. A detailed view of the South Pacific id from satellite altimetry. J. Geophys. Res., 89: 89–1104.
ell, D.T., 1984b. Along-track deflection of the vertical m SEASAT: GEBCO overlays. Natl. Oceanic Atmos. lm. Tech. Memo. NOS NGS-40.
ell, D.T. and McAdoo, D.C., in press. Marine gravity of Southern Ocean and Antarctic margin from GEOSAT. Geophys. Res.
tava, S.P. and Tapscott, C.R., 1986. Plate kinematics of North Atlantic. In: P.R. Vogt and B.E. Tucholke (Eds), The Geology of North America. Vol. M, The Western North Atlantic Region. (A Decade of North American Geology.) Geol. Soc. Am., Boulder, Colo., pp. 379–404.
Tapley, B.D., Born, G.H. and Parke, M.E., 1982. The SEASAT altimeter data and its accuracy assessment. J. Geophys. Res., 87: 3179–3188.
Van Hee, D.H., 1987. Preliminary results from the processing of a limited set of GEOSAT radar altimeter data. John Hopkins Appl. Phys. Lab. Tech. Dig., 8: 201–205.
Weissel, J.K. and Hayes, D.E., 1972. Magnetic anomalies in the southeast Indian Ocean. In: D.E. Hayes (Editor), Antarctic Oceanology II: the Australian–New Zealand Sector. Antarct. Res. Ser., 19: 165–196.
Weissel, J.K., Anderson, R.N. and Geller, C.A., 1980. Deformation of the Indo-Australian plate. Nature, 287: 284–291.

Tectonophysics, 155 (1988) 27–48
Elsevier Science Publishers B.V., Amsterdam – Printed in The Netherlands

Plate tectonic reconstructions of the Cretaceous and Cenozoic ocean basins

CHRISTOPHER R. SCOTESE [1], LISA M. GAHAGAN [2] and ROGER L. LARSON [3]

[1] *Shell Development Co., Bellaire Research Center, P.O. Box 481, Houston, TX 77001 (U.S.A.)*
[2] *The Department of Geological Sciences, The University of Texas, Austin, TX 78713 (U.S.A.) and The Institute for Geophysics, University of Texas, Austin, TX 78759 (U.S.A.)*
[3] *School of Oceanography, University of Rhode Island, Kingston, RI 02881 (U.S.A.)*

(Received May 18, 1987; revised version accepted September 8, 1987)

Abstract

Scotese, C.R., Gahagan, L.M. and Larson, R.L., 1988. Plate tectonic reconstructions of the Cretaceous and Cenozoic ocean basins. In: C.R. Scotese and W.W. Sager (Editors), Mesozoic and Cenozoic Plate Reconstructions. *Tectonophysics*, 155: 27–48.

In this paper we present nine reconstructions for the Mesozoic and Cenozoic, based on previously published sea-floor spreading isochrons*. The purpose of this study was (1) to determine if the isochrons could be refitted to produce accurate plate tectonic reconstructions, (2) to identify areas of apparent mismatch between magnetic isochrons as a focus for further investigations, and (3) to test the capabilities and accuracy of interactive computer graphic methods of plate tectonic reconstruction. In general, Tertiary and Late Cretaceous isochrons could be refitted with little overlap and few gaps; however, closure errors were apparent in the vicinity of the Bouvet and Macquarie triple junctions. It was not possible to produce Early Cretaceous reconstructions that were consistent with the previously published isochrons. In this paper we also propose that the Late Cretaceous and Early Tertiary plate reorganizations observed in the Indian Ocean were the result of the progressive subduction of an intra-Tethyan rift system.

Introduction

In 1985 a map illustrating the age of the ocean basins and continents was published by Larson et al. (1985) (Fig. 1), on which the oceans were divided into colored regions bounded by magnetic isochrons representing the following geologic time intervals: Pleistocene (chron 2, 1.9 Ma), Pliocene (chron 3a, 5.9 Ma), Miocene (chron 6b, 23 Ma), Oligocene (chron 15, 37.7 Ma), Eocene (chron 25, 59.2 Ma), Paleocene (chron 29, 66.2 Ma), Late Cretaceous (chron 34, 84.0 Ma), Middle Cretaceous (chron M0, 118.7 Ma) and Early Cretaceous (chron M17, 143.8 Ma). The isochrons were drawn using published and unpublished magnetic anomalies and bathymetric information, and were modified to take into account new data from Seasat altimetry (Haxby, 1985). This map supercedes the maps of the age of the ocean floor published by Pitman III et al. (1974) and Sclater et al. (1981).

In this study, we have used interactive computer graphics to produce plate tectonic reconstructions for each of the sea-floor spreading isochrons described by Larson et al. (1985). The goals of this investigation were (1) to determine if the isochrons mapped by Larson et al. could be

* Larson et al. (1985).

0040-1951/88/$03.50

rinct geoid highs; in areas where there are mass
icits, such as trenches or deep fracture zone
leys, there are corresponding geoid lows. This
ct correlation between the short-wavelength
tures (or high-frequency component) of the ge-
and the bathymetry of the ocean floor (Haxby
l., 1983; Sandwell, 1984a) has been success-
y used to identify and locate a variety of
hymetric features. Geoid data, as collected by
llite, have yielded information on trenches
Adoo, 1981), on the location of fracture zones
he Pacific (Sailor and Okal, 1983) and Atlantic
nde et al., in press) oceans, and on the global
ersal of seamounts (Craig and Sandwell, in
s).

n this paper we present a global map (Fig. 1),
d on measurements of the high-frequency
ponent of the geoid that defines the trends
outlines of tectonic features on the ocean
r. This map can be used to identify oceanic
ture zones, active and extinct spreading ridges,
nounts, trenches and aseismic volcanic edifices,
ell as some of the aspects of the structure of
ly buried basement features along rifted con-
ntal margins. The lineations on the map that
espond to fracture zones record the movement
he plates through time and thus serve as
nic "flowlines" between the plates. These
lines, together with the other features on the
, reveal how the tectonic history of the ocean
ns has been woven into the ocean floor itself,
thus reveal what we refer to as the "tectonic
c" of the ocean basins.

ur results, though similar to the work of Haxby
7), were obtained by a different technique.
er than work with gridded, areal averages
by, 1987), our interpretation is based on a
t analysis of individual measurements. By
ing with discrete data points, we have been
to increase the resolution of our interpreta-
and map previously unknown tectonic fea-
, as well as resolve the shape of known tectonic
res in greater detail.

the following sections we outline the meth-
that we have used to analyze the satellite
etry data. This includes a brief discussion of
processing of the satellite altimetry data as
as the techniques that were used to produce
the map (Fig. 1). In the first part of the discussion section, guidelines are given that enable the reader to identify the distinctive geoid signals that accompany ridges, trenches, fracture zones, etc. In the second part of the discussion section, some of the major tectonic features that we have mapped are described. This section includes a discussion of the correlation between our interpretations and known bathymetric features, as well as a description of some of the previously unmapped, tectonic features that have been revealed by satellite altimetry data. In the conclusion, we discuss how the tectonic fabric map of the ocean basins is being used to produce plate reconstructions and how it might be used to provide insights into the kinematics of the plate tectonic process.

Methods

SEASAT and GEOSAT missions

In June, 1978, NASA launched the SEASAT satellite to collect data which would provide information on oceanic parameters such as the height of the sea surface, wave height and sea-surface winds (Lame and Born, 1982). While ground-tracking lasers located the satellite in its orbit, the satellite used a radar altimeter to measure the altitude between itself and the sea surface (h) (Fig. 2). After instrument, atmospheric and geophysical corrections were made to h, this distance was subtracted from the distance between the satellite and a reference ellipsoid for the Earth (h^*). The difference between h^* and h is the height of the sea surface (h_g) (Fig. 2).

During its 3 months of operation, the SEASAT satellite collected more than 4 million data points (Sandwell, 1984b). The satellite, possessing a footprint of 2–5 km in diameter, made altimetry measurements ten times per second. These were averaged into one point per second. The SEASAT satellite obtained several global data sets with a 165 km equatorial spacing of ground tracks and a 3 day repeat-orbit set with a 900 km equatorial spacing of ground tracks (Tapley et al., 1982). Data were collected along both ascending orbital tracks (trending SE–NW) and descending orbital tracks (trending NE–SW).

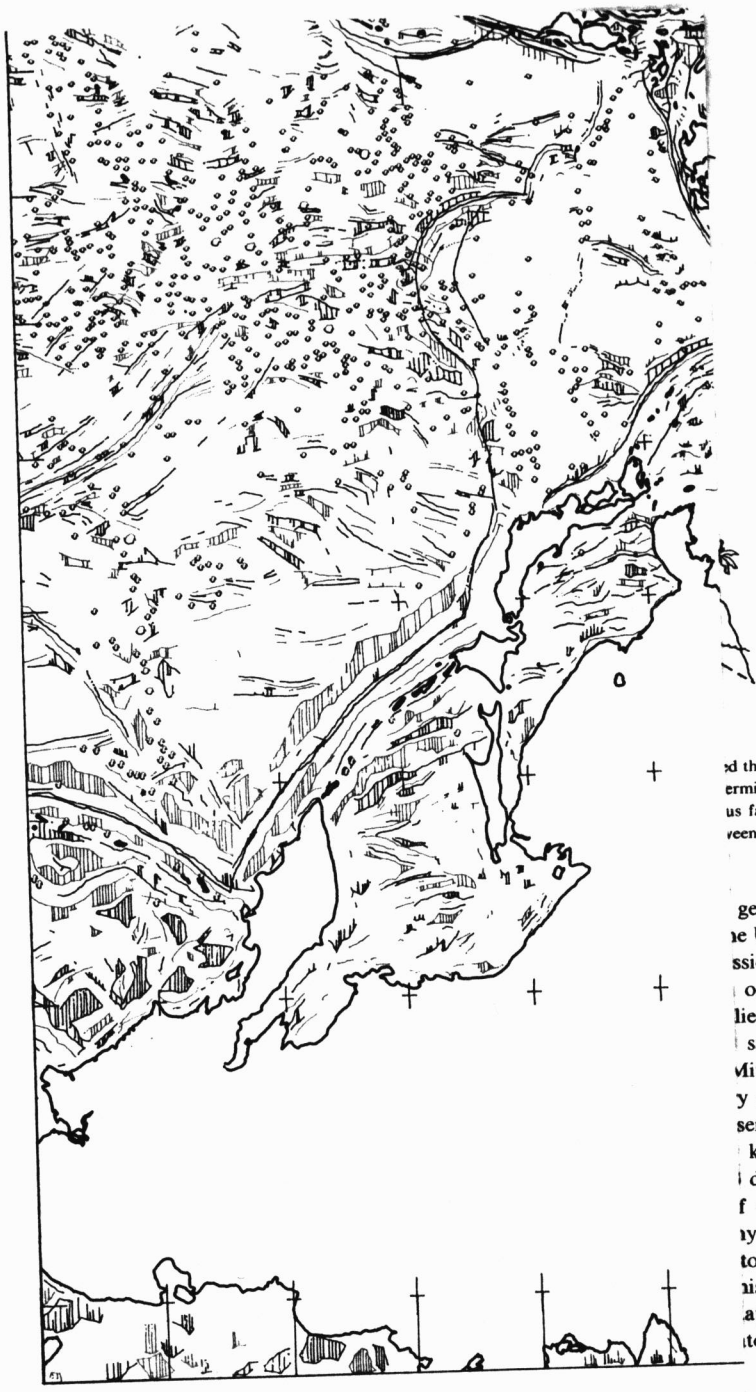

d the distance (h) between
ermitting the calculation of
us factors (instrument and
veen h^* and h.

geodesy satellite, or
ne U.S. Navy in order
ssion and obtain a
oceanographic data
lied Physics Labora-
satellite and is re-
Mitchell et al., 1987).
y mission, GEOSAT
servations along an
km. The orbits re-
days and the tracks
f 4 km (Jenson and
ny and Kilgus, 1987;
tober 1, 1986, GEO-
ission of collecting
ata along a 17 day
torial-spaced ground